Miniband Bloch transport through a one-dimensional semiconductor superlattice

1992 J. Phys.: Condens. Matter 4 9367

(http://iopscience.iop.org/0953-8984/4/47/017)

J. Phys.: Condens. Matter 4 (1992) 9367–9374. Printed in the UK

Miniband Bloch transport through a one-dimensional semiconductor superlattice

X L Lei

Chinese Centre of Advanced Science and Technology (World Laboratory), PO Box 8730, Beijing 100080, People's Republic of China
and
Shanghai Institute of Metallurgy, Chinese Academy of Sciences, 865 Changning Road, Shanghai 200050, People's Republic of China†

Received 11 May 1992, in final form 26 August 1992

Abstract. The balance-equation theory recently developed for miniband Bloch transport in semiconductor superlattices is extended to systems with a strong lateral confinement. Carrier statistics, electron heating, and realistic scattering mechanisms due to impurities and phonons are included in the force- and energy-balance equations. Impurity- and phonon-limited linear mobilities are investigated as functions of the carrier occupation and temperature. The non-linear behaviour of the drift velocity against electric field for these one-dimensional superlattices, derived from the balance-equation theory, exhibits features different from that of a three-dimensional superlattice, but similar to the predictions of the Esaki–Tsu and Boltzmann theories.

1. Introduction

Recent technological advances in semiconductor microfabrication, which have made it possible to confine electrons to regions with a lateral extent of order of 100 nm or less, have stimulated growing interest in electron transport through a string of coupled quantum dots or a one-dimensional semiconductor superlattice [1, 2]. Experimental and theoretical studies have so far concentrated mainly on its ballistic transport properties at very low temperatures, when elastic and inelastic scatterings can be avoided and quantum coherence and related phenomena are expected to show up. On the other hand, carrier conduction of the Esaki–Tsu type [3] through a one-dimensional superlattice, which is subject to impurity and phonon scatterings, is also of great interest.

There are two different types of theories for superlattice miniband transport. The earliest model of Esaki and Tsu [3], considering a single electron moving in a one-dimensional miniband of width Δ with a constant scattering time τ, gave a simple relation between the drift velocity v_d and the electric field E:

$$v_d = v_p \frac{2E/E_c}{1+(E/E_c)^2} \tag{1}$$

where $E_c = 1/e\tau d$, $v_p = \Delta d/4$, and d is the period of the superlattice. This formula states that the drift velocity reaches its maximum v_p at a field equal to the

† Mailing address.

0953-8984/92/479367+08$07.50

critical value E_c, and that when $E > E_c$ the drift velocity decreases with increasing electric field, i.e. the negative differential velocity. Later, more careful solutions of the Boltzmann equation with one (elastic) scattering time [4–6] or with two (elastic and inelastic) scattering times [7–9] yielded, except for the expression of v_p, the same dependence of v_d/v_p as a function of E/E_c, independent of the superlattice period, miniband width, scattering times and temperature.

On the other hand, the balance-equation theory recently developed [10, 11] for carrier miniband transport in a three-dimensional superlattice with realistic impurity scattering and electron–phonon interactions, predicts a widely varying temperature- and miniband-width-dependent non-linear velocity-field behaviour [12]. Since theories of the Esaki–Tsu–Boltzmann (ETB) type developed so far deal essentially with one-dimensional models using a constant scattering-time approximation, it is not clear whether the distinct predictions for the velocity-field behaviour from these two types of theories are intrinsic in nature, or result from the dimensionality difference of the systems they deal with, or from the constant scattering-time approximation used by the former.

The purpose of this paper is to extend the balance-equation theory for the miniband Bloch transport to a one-dimensional superlattice with realistic impurity and phonon scatterings, and to study the effect of the carrier confinement on its miniband transport. The results will be compared with Esaki–Tsu and Boltzmann theories.

2. Balance equations for a 1D superlattice

Consider a model superlattice system along the z direction, which is formed by periodical potential wells and barriers of finite height. In the x–y plane there exists an infinitely high potential wall such that electrons are confined in a small cylindrical region of diameter d_r. The single-electron state of the system can be described by transverse quantum numbers l, a longitudinal miniband index n and a longitudinal wavevector k_z ($-\pi/d < k_z \leqslant \pi/d$, where d is the period of the superlattice).

We assume that the energy separation between the transverse ground and excited states, and the energy gap between the longitudinal lowest and second minibands, are large enough; then only the transverse ground state and the longitudinal lowest miniband need be taken into consideration. We thus have a quasi-1D system, the state of which can be described by simply a one-dimensional wavevector k_z, with the energy dispersion, under the tight-binding approximation, expressed in the form

$$\varepsilon(k_z) = (\Delta/2)(1 - \cos k_z d) \tag{2}$$

where Δ is the miniband width.

When a uniform electric field E is applied parallel to the superlattice axis, the carriers are accelerated by the field and scattered by impurities and by phonons, resulting in an overall drift motion and possible heating of the carrier system. Such a transport state of the system is described in the balance-equation theory by the centre-of-mass (CM) momentum $P_d \equiv N p_d$ (where N is the total number of carriers) and the relative electron temperature T_e, and they are determined by the effective force- and energy-balance equations [10, 11]:

$$\mathrm{d}v_d/\mathrm{d}t = eE/m_z^* + A_i + A_p \tag{3}$$

$$\mathrm{d}h_e/\mathrm{d}t = eEv_d - W. \tag{4}$$

In the above

$$v_d = \frac{2}{N}\sum_{k_z} v(k_z) f(\bar{\varepsilon}(k_z), T_e) \tag{5}$$

(where $v(k_z) = d\varepsilon(k_z)/dk_z$ is the velocity function in the z direction) is the centre-of-mass velocity, i.e. the average drift velocity of the carriers, and h_e is the average electron energy per carrier. Furthermore

$$\frac{1}{m_z^*} = \mathcal{K}_{zz} = \frac{2}{N}\sum_{k_z} \frac{d^2\varepsilon(k_z)}{dk_z^2} f(\bar{\varepsilon}(k_z), T_e) \tag{6}$$

is an ensemble-averaged inverse effective-mass, introduced to describe the response of the electron system to an external field. In the above equations

$$f(\bar{\varepsilon}(k_z), T_e) \equiv \{\exp(\bar{\varepsilon}(k_z) - \mu)/T_e] + 1\}^{-1} \tag{7}$$

is the Fermi distribution function at the electron temperature T_e, μ is the chemical potential determined by the condition

$$N = 2\sum_{k_z} f(\bar{\varepsilon}(k_z), T_e) \tag{8}$$

and

$$\bar{\varepsilon}(k_z) \equiv \varepsilon(k_z - p_d) \tag{9}$$

is the relative electron energy.

Assuming that impurities are randomly distributed in the background and phonons are three-dimensional bulk modes, we can write the impurity- and phonon-induced frictional accelerations, A_i and A_p, and the energy-transfer rate from the electron system to the phonon system, W, in the following form:

$$A_i = \frac{2\pi n_i}{N}\sum_{k_z,q} |u(q)|^2 |J(q_x, q_y)|^2 |g(q_z)|^2 [v(k_z + q_z) - v(k_z)] \times \delta(\varepsilon(k_z + q_z) - \varepsilon(k_z)) \frac{f(\bar{\varepsilon}(k_z), T_e) - f(\bar{\varepsilon}(k_z + q_z), T_e)}{|\epsilon(q, \bar{\varepsilon}(k_z) - \bar{\varepsilon}(k_z + q_z))|^2} \tag{10}$$

$$A_p = \frac{4\pi}{N}\sum_{k_z,q,\lambda} |M(q,\lambda)|^2 |J(q_x, q_y)|^2 |g(q_z)|^2 [v(k_z + q_z) - v(k_z)] \times \delta(\varepsilon(k_z + q_z) - \varepsilon(k_z) + \Omega_{q,\lambda}) \frac{f(\bar{\varepsilon}(k_z), T_e) - f(\bar{\varepsilon}(k_z + q_z), T_e)}{|\epsilon(q, \bar{\varepsilon}(k_z) - \bar{\varepsilon}(k_z + q_z))|^2} \times \left[n\left(\frac{\Omega_{q,\lambda}}{T}\right) - n\left(\frac{\bar{\varepsilon}(k_z) - \bar{\varepsilon}(k_z + q_z)}{T_e}\right)\right] \tag{11}$$

$$W = \frac{4\pi}{N}\sum_{k_z,q,\lambda} |M(q,\lambda)|^2 |J(q_x, q_y)|^2 |g(q_z)|^2 \Omega_{q,\lambda} \delta(\varepsilon(k_z + q_z) - \varepsilon(k_z) + \Omega_{q,\lambda}) \times \frac{f(\bar{\varepsilon}(k_z), T_e) - f(\bar{\varepsilon}(k_z + q_z), T_e)}{|\epsilon(q, \bar{\varepsilon}(k_z) - \bar{\varepsilon}(k_z + q_z))|^2} \times \left[n\left(\frac{\Omega_{q,\lambda}}{T}\right) - n\left(\frac{\bar{\varepsilon}(k_z) - \bar{\varepsilon}(k_z + q_z)}{T_e}\right)\right]. \tag{12}$$

Here $u(q)$ is the 3D Fourier transform of the impurity potential and $M(q,\lambda)$ is the 3D plane-wave representation of the electron–phonon matrix element for phonons of wavevector q in branch λ, having frequency $\Omega_{q,\lambda}$; $n(x) \equiv (e^x - 1)^{-1}$ is the Bose function and $\epsilon(q,\omega)$ is the dielectric function of electrons in the random-phase approximation. In these equations $J(q_x, q_y)$ is a form factor due to the confinement of the lateral ground-state wavefunction $\phi(x,y)$:

$$J(q_x, q_y) = \int\int \mathrm{d}x\mathrm{d}y|\phi(x,y)|^2 e^{i(q_x x + q_y y)} \tag{13}$$

and $g(q_z)$ is a form factor determined by the wavefunction of the superlattice miniband. In the extreme tight-binding limit for the envelope function it is simply the form factor of a single quantum well: $g(q_z) = d^{-1}\int \mathrm{d}z|\phi(z)|^2 \exp(iq_z z)$, where $\phi(z)$ is the single-well function.

3. Temperature variations of the Fermi level and effective mass

In terms of the electron density per unit line along the z direction, N_1, equation (8) for the determination of the Fermi energy can be written as

$$N_1 d = \frac{1}{\pi}\int_{-\pi}^{\pi} \frac{\mathrm{d}z}{\exp\{[(\Delta/2)(1-\cos z) - \mu]/T_e\} + 1}. \tag{14}$$

The zero-temperature Fermi level, $\varepsilon_f^0 \equiv \mu(0)$, is given by

$$\frac{2\varepsilon_f^0}{\Delta} = 1 - \cos(\tfrac{1}{2}\pi N_1 d). \tag{15}$$

This limit is valid when $\Delta/2T_e \gg 1$. In the opposite limit, $\Delta/2T_e \ll 1$, we have

$$\mu/T_e \simeq -\ln(2/N_1 d - 1) + \Delta/2T_e. \tag{16}$$

Note that the maximum number of electrons the lowest miniband can accommodate is $N_1 d = 2$. Equation (16) shows that in the high-temperature limit μ/T_e approaches a constant, $-\ln(2/N_1 d - 1)$, which is negative when $N_1 d < 1$ and positive when $N_1 d > 1$. The non-degenerate (Maxwell–Boltzmann) limit thus does not generally exist in this system, except for very small $N_1 d \sim 0$, such that $\ln(2/N_1 d - 1) \gg 1$. When $N_1 d = 1$ (half filled), the Fermi level $\mu = \mu(0) = \Delta/2$, does not vary with temperature. The average drift velocity and the inverse effective-mass of the system can be expressed as

$$v_d = v_m \alpha_T^{(1)} \sin(p_d d) \tag{17}$$

$$\frac{1}{m^*} = \frac{1}{M^*}\alpha_T^{(1)} \cos(p_d d) \tag{18}$$

with $v_m = \Delta d/2$, $1/M^* = \Delta d^2/2$, and

$$\alpha_T^{(1)} = \frac{1}{\pi N_1 d}\int_{-\pi}^{\pi} \frac{\cos z\,\mathrm{d}z}{\exp\{[(\Delta/2)(1-\cos z) - \mu]/T_e\} + 1} \tag{19}$$

is a temperature-dependent coefficient. In the low-temperature limit

$$\alpha_T^{(1)} = \sin(\tfrac{1}{2}\pi N_1 d)/(\tfrac{1}{2}\pi N_1 d) \tag{20}$$

and at high temperatures, $\Delta/2T_e \ll 1$, we have

$$\alpha_T^{(1)} = (1 - N_1 d/2)(\Delta/4T_e). \tag{21}$$

4. Linear mobilities

The steady-state version of the balance equations (3) and (4) determines the DC drift velocity and the electron temperature under the influence of a constant electric field along the z direction. In the weak electric-field limit these equations require $T_e = T$, and the inverse linear mobility $1/\mu$ equals the sum of the impurity and phonon contributions:

$$1/\mu = 1/\mu_i + 1/\mu_p \tag{22}$$

in which the impurity-induced inverse mobility $1/\mu_i$ is given by

$$\frac{1}{\mu_i} = \frac{n_i}{2\pi e N_1 d^2 (\alpha_T^{(1)})^2} \int\int dk_z dq_z |\tilde{u}(q_z)|^2 |g(q_z)|^2 [\sin(k_z + q_z)d - \sin(k_z d)]^2 \times \left(-\frac{\partial f(\varepsilon(k_z), T)}{\partial \varepsilon(k_z)}\right) \delta(\varepsilon(k_z + q_z) - \varepsilon(k_z)) \tag{23}$$

where n_i is the impurity density, $|\tilde{u}(q_z)|^2$ is an effective one-dimensional impurity potential obtained from a statically screened and form-factor-weighted 3D plane-wave representation of the impurity potential $|u(q)|^2$:

$$|\tilde{u}(q_z)|^2 = \int\int \frac{dq_x dq_y}{(2\pi)^2} \frac{|u(q)|^2}{|\epsilon(q, 0)|^2} |J(q_x, q_y)|^2. \tag{24}$$

The inverse mobility induced by the λ-branch phonons is given by

$$\frac{1}{\mu_{p\lambda}} = -\frac{1}{\pi e N_1 d^2 T (\alpha_T^{(1)})^2} \int\int dk_z dq_z \int\int \frac{dq_x dq_y}{(2\pi)^2} |\tilde{M}(q, \lambda)|^2 |J(q_x, q_y)|^2 |g(q_z)|^2 \times [\sin(k_z + q_z)d - \sin(k_z d)]^2 \delta(\varepsilon(k_z + q_z) - \varepsilon(k_z) + \Omega_{q,\lambda}) \times [-n'(\Omega_{q,\lambda}/T)][f(\varepsilon(k_z), T) - f(\varepsilon(k_z) - \Omega_{q,\lambda}, T)] \tag{25}$$

with $\tilde{M}(q, \lambda) \equiv M(q, \lambda)/\epsilon(q, \Omega_{q,\lambda})$ being the screened electron–phonon matrix element.

Carrying out the integration over k_z in (23) to eliminate the δ function, we can express the impurity-limited linear mobility in the form

$$\frac{1}{\mu_i} = \frac{n_i}{e N_1 d^3 \Delta T (\alpha_T^{(1)})^2} \int \frac{dq_z}{\pi} |\tilde{u}(q_z)|^2 |g(q_z)|^2 |\sin(\tfrac{1}{2} q_z d)| \times \left(\frac{e^{\nu_+}}{(e^{\nu_+} + 1)^2} + \frac{e^{\nu_-}}{(e^{\nu_-} + 1)^2}\right) \tag{26}$$

with

$$\nu_\pm = \frac{\Delta}{2T}[1 \pm \cos(q_z d/2)] - \frac{\mu}{T}. \tag{27}$$

Due to the existence of the form factor $|g(q_z)|^2$, the dominant contribution to the integral in (26) comes from $|q_z| \leqslant \pi/d$. To see the explicit dependence of $1/\mu_i$ on the electron density, miniband width and superlattice period, we assume that $|\tilde{u}(q_z)|^2$ can be approximately treated as a constant $\tilde{u}^2$. In the degenerate limit we thus have

$$\frac{1}{\mu_i} = \frac{4\pi n_i \tilde{u}^2}{e d^3 \Delta^2} \frac{N_1 d}{\sin^2(\pi N_1 d/2)} C_z. \tag{28}$$

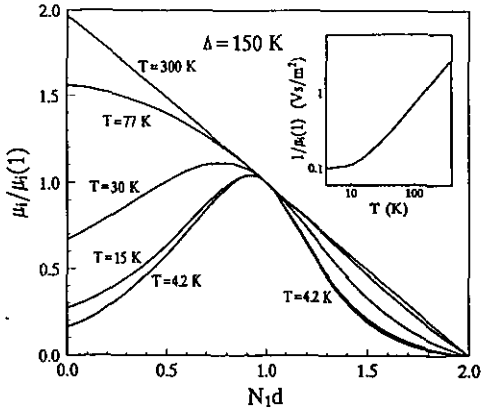

Figure 1. Impurity-limited low-field mobility μ_i normalized by its value at $N_1d = 1$, $\mu_i(1)$, is shown as a function of N_1d at temperatures $T = 4.2$, 15, 30, 77 and 300 K, for a 1D superlattice of period $d = 150$ Å and miniband width $\Delta = 150$ K. The inset gives $1/\mu_i(1)$ values as a function of temperature.

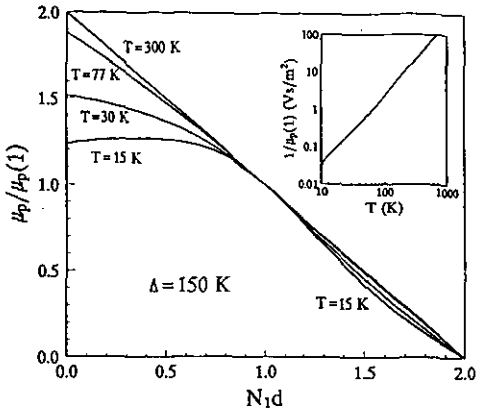

Figure 2. Acoustic-phonon-limited low-field mobility μ_p normalized by its value at $N_1d = 1$, $\mu_p(1)$, is shown as a function of N_1d at temperatures $T = 15$, 30, 77 and 300 K, for a 1D superlattice of period $d = 150$ Å and miniband width $\Delta = 150$ K. The inset gives $1/\mu_p(1)$ values as a function of temperature.

The constant C_z, being of order of one, depends on the form factor. This equation is valid if $\epsilon_f^0/T \ll 1$.

At high temperatures, $\Delta/2T_c \ll 1$, the impurity-induced inverse mobility can be written as

$$\frac{1}{\mu_i} = \frac{64}{\pi}\frac{n_i\tilde{u}^2}{ed^3\Delta^2}\frac{T}{\Delta}\frac{C_h}{(1 - N_1d/2)} \tag{29}$$

where

$$C_h = \frac{1}{4}\int dy|g(y/d)|^2|\sin(y/2)| \tag{30}$$

is also a constant of order of one. If $|g(q_z)|^2 = 1$ for $|q_z| \leqslant \pi/d$ and $|g(q_z)|^2 = 0$ otherwise, we have both $C_z = 1$ and $C_h = 1$. Equations (29) and (30) indicate that in a one-dimensional superlattice, the impurity-limited linear mobility varies strongly with the miniband occupation. At zero temperature the mobility approaches zero when $N_1d \to 0$ or $N_1d \to 2$, and the highest mobility is reached at $N_1d \sim 0.8$. This behaviour is a consequence of Fermi statistics and the finite miniband width. For the case of $N_1d = 2$, i.e. a filled miniband, the mobility of course vanishes. At low temperatures only a small part of the total carriers around the Fermi level contributes to the transport. The percentage of the carriers taking part in the conduction reaches a maximum in the case of a half-filled miniband, resulting in a mobility maximum around $N_1d = 1$. With the rise in temperature an increasing percentage of the carriers takes part in the conduction, especially for small N_1d, leading to a diminishing of the mobility maximum. At high temperatures the mobility decreases monotonically with increasing N_1d and approaches zero when $N_1d \to 2$.

The impurity-limited linear mobilities μ_i at several lattice temperatures, normalized separately by their values at $N_1d = 1$, $\mu_i(1)$, are plotted in figure 1

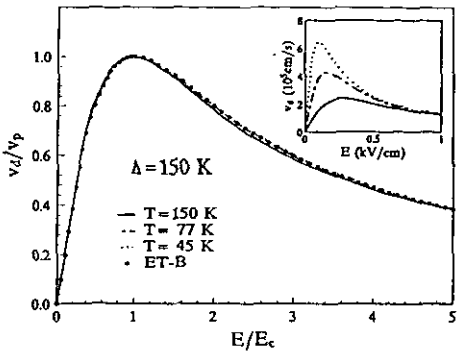

Figure 3. Drift velocity v_d normalized to its peak value v_p is plotted as a function of the normalized field E/E_c, calculated from the balance equations (3) and (4), respectively at lattice temperature $T = 45$, 77 and 150 K, for a 1D superlattice of $d = 150$ Å, $\Delta = 150$ K, $N_1 d = 0.9$ and low-field inverse mobility $1/\mu = 0.1\,\mathrm{V\,s\,m^{-2}}$ at temperature $T = 4.2$ K. The peak drift velocities and critical fields are $v_p = 6.5 \times 10^5\,\mathrm{cm\,s^{-1}}$ and $E_c = 102\,\mathrm{V\,cm^{-1}}$ for the $T = 45$ K curve, $v_p = 4.3 \times 10^5\,\mathrm{cm\,s^{-1}}$ and $E_c = 155\,\mathrm{V\,cm^{-1}}$ for the $T = 77$ K curve, and $v_p = 2.4 \times 10^5\,\mathrm{cm\,s^{-1}}$ and $E_c = 280\,\mathrm{V\,cm^{-1}}$ for the $T = 150$ K curve. The dots in the figure represent the behaviour of equation (1). The inset shows v_d against E for these systems.

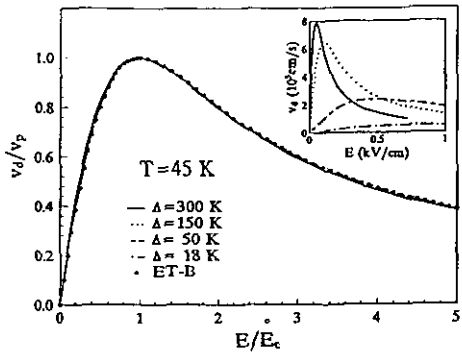

Figure 4. v_d/v_p is plotted as a fuction of E/E_c at lattice temperature $T = 45$ K, for four 1D GaAs superlattice systems having the same period $d = 150$ Å, $N_1 d = 0.9$ and low-temperature (4.2 K) linear inverse mobility $1/\mu = 0.1\,\mathrm{V\,s\,m^{-2}}$, but different miniband widths $\Delta = 18$, 50, 150 and 300 K. The peak drift velocities and the critical fields are $v_p = 5.4 \times 10^4\,\mathrm{cm\,s^{-1}}$ and $E_c = 900\,\mathrm{V\,cm^{-1}}$ for the $\Delta = 18$ K system, $v_p = 2.4 \times 10^5\,\mathrm{cm\,s^{-1}}$ and $E_c = 480\,\mathrm{V\,cm^{-1}}$ for the $\Delta = 50$ K system, $v_p = 6.5 \times 10^5\,\mathrm{cm\,s^{-1}}$ and $E_c = 102\,\mathrm{V\,cm^{-1}}$ for the $\Delta = 150$ K system, and $v_p = 7.9 \times 10^5\,\mathrm{cm\,s^{-1}}$ and $E_c = 46\,\mathrm{V\,cm^{-1}}$ for the $\Delta = 300$ K system. The dots in the figure represent the behaviour of equation (1). The inset shows v_d against E for these systems.

for a one-dimensional superlattice of transverse confinement $d_r = 100$ Å, period $d = 150$ Å, miniband width $\Delta = 150$ K, and impurity-induced low-field inverse mobility $1/\mu_i(1) = 0.1\,\mathrm{V\,s\,m^{-2}}$ at temperature $T = 4.2$ K. These curves are obtained from (26) by assuming a constant $|\tilde{u}(q_z)|^2$. The q_z dependence of $\tilde{u}(q_z)$ of course affects the behaviour of the mobility against $N_1 d$.

Figure 2 shows the low-field mobility limited by the longitudinal and transverse acoustic phonon scatterings (through both the deformation potential and the piezoelectric couplings) as a function of $N_1 d$ for the same 1D GaAs superlattice as described above. The mobility is calculated from (25) assuming three-dimensional bulk phonon modes and using standard electron–phonon matrix element and typical parameters for GaAs [13].

5. Non-linear velocity-field behaviour

The steady-state non-linear drift velocity, v_d, has been calculated as a function of the electric field E from the steady-state version of the balance equations (3) and (4) for several 1D GaAs superlattices. Scatterings due to charged impurities, acoustic phonons (interacting with electrons through deformation and piezoelectric potentials) are taken into account. Optic phonons do not contribute to intra-miniband electron transitions when the miniband width Δ is smaller than the optic phonon energy, and thus play no role in the case we are discussing. In figure 3 we plot the

normalized drift velocity v_d/v_p as a function of the normalized electric field E/E_c at lattice temperatures $T = 45$, 77 and 150 K, for a 1D superlattice of $d_r = 100$ Å, $d = 150$ Å, $\Delta = 150$ K, $N_1 d = 0.9$ and low-field inverse mobility $1/\mu = 0.1\,\mathrm{V\,s\,m^{-2}}$ at temperature $T = 4.2$ K. The behaviour predicted by the Esaki–Tsu and Boltzmann theories, equation (1), is shown in this figure as dots.

In figure 4 we plot v_d/v_p against E/E_c at lattice temperature $T = 45$ K, for four GaAs-based one-dimensional superlattices having the same transverse confinement $d_r = 100$ Å, period $d = 150$ Å, $N_1 d = 0.9$ and low-temperature (4.2 K) linear inverse mobility $1/\mu = 0.1\,\mathrm{V\,s\,m^{-2}}$, but with different miniband widths $\Delta = 18$, 50, 150 and 300 K. Also shown as dots in this figure are the predictions from (1).

The striking feature is that, in all the 1D superlattices investigated, the normalized v_d/v_p–E/E_c behaviour is very closed to that of equation (1) given by the Esaki–Tsu and Boltzmann theories, although their velocity–field curves appear quite distinct (see the insets of figures 3 and 4). This is in contrast with the three-dimensional case, where the balance-equation theory yields a variable behaviour [12] for v_d/v_p against E/E_c.

Acknowledgments

The author wishes to thank the National Natural Science Foundation of China for support of this work.

References

[1] Ulloa S E, Castaño E and Kirczenow G 1990 *Phys. Rev.* B **41** 12350; **42** 3753
[2] Haug R J, Hong J M and Lee K Y 1992 *Surf. Sci.* **263** 415
[3] Esaki L and Tsu R 1970 *IBM J. Res. Dev.* **14** 61
[4] Lebwohl P A and Tsu R 1970 *J. Appl. Phys.* **41** 2664
[5] Shik A Ya 1973 *Sov. Phys.–Semicond.* **7** 187
[6] Suris R A and Shchamkhalova B S 1984 *Sov. Phys.–Semicond.* **18** 738
[7] Ktitorov S A, Simin G S and Sindalovskii V Ya 1972 *Sov. Phys.–Solid State* **13** 1872
[8] Ignatov A A and Shaskin V I 1983 *Phys. Lett.* **94A** 169
[9] Ignatov A A, Dodin E P and Shaskin V I 1991 *Mod. Phys. Lett.* B **5** 1187
[10] Lei X L, Horing N J M and Cui H L 1991 *Phys. Rev. Lett.* **66** 3277
[11] Lei X L 1992 *Phys. Status Solidi b* **170** 519
[12] Lei X L and da Cunha Lima I C 1992 *J. Appl. Phys.* **71** 5517
[13] Lei X L, Birman J L and Ting C S 1985 *J. Appl. Phys.* **58** 2270